ARTICLE

High Pressure Phase Stability of Ti with Self-consistent *ab initio* Lattice Dynamics Approach

Zhao-yi Zeng[a,b*], Cui-e Hu[a,b], Xun Liu[c], Zhang Wei[b], Ling-cang Cai[b]

a. College of Physics and Electronic Engineering, Chongqing Normal University, Chongqing 400047, China
b. National Key Laboratory for Shock Wave and Detonation Physics Research, Institute of Fluid Physics, Chinese Academy of Engineering Physics, Mianyang 621900, China
c. Institute of Pulsed Power Science, Kumamoto University, Kurokami, Kumamoto 860-8555, Japan

(Dated: Received on November 11, 2014; Accepted on February 15, 2015)

The traditional quasiharmonic approximation cannot predict the phase diagram of Ti accurately, due to the well-known soften phonon modes of the β-Ti. By means of self-consistent *ab initio* lattice dynamics (SCAILD) method, in which the effects of phonon-phonon interactions are considered, the phonon dispersion relations at finite temperature for Ti are calculated. From the phonon dispersions, we extrapolat the acoustic velocities and harmonic elastic constants. The dynamical stable regions and phase diagram of Ti are also predicted successfully. The results show that SCAILD method can be designed to work for strongly anharmonic systems where the QHA fails.

Key words: Transition metal, Lattice dynamics, Phase transition, Density functional theory

I. INTRODUCTION

In the past decades, density functional theory (DFT) has successfully predicted the thermodynamic properties and phase transformations for elemental and alloyed materials. Though it is a ground-state theory, the crucial effect of thermal vibrations of atoms in principle can be included via the so-called quasiharmonic approximation (QHA). QHA is widely used to describe the thermal properties of solid under high temperature and high pressure, it assumes that the potential energy surface does not depend on temperature and the intrinsic anharmonic effects are neglected. In particular, it becomes problematic when the high temperature phase is mechanically unstable at low temperatures, *i.e.*, the phonon spectra contain imaginary frequencies but stabilized due to the anharmonic contributions to the free energy at elevated temperatures. To resolve this problem, the anharmonic effects of high temperature should be considered firstly. In principle, *ab initio* molecular dynamics is a good choice. However, the computational cost of *ab initio* molecular dynamics simulations limits the applicability. Thus, there is significant motivation to develop a simplified method of dealing with mechanically unstable systems. The self-consistent *ab initio* lattice dynamics (SCAILD) method is such a convenient and reliable method [1−4]. As the interaction between phonons can be considered in SCAILD method, the influence of anharmonic contribution to the lattice dynamics can be investigated as a function of temperature. By using this method, the phonon dispersions of group IV metals were reproduced and the transition temperatures between different phases were also obtained at zero pressure [4].

As a well-known strongly anharmonic solid, titanium (Ti) has been investigated extensively. Ti exhibits a phase transition from the ground-state hexagonal close-packed (hcp or α phase, space group $P6_3/mmc$) crystal structure to the body-centered cubic (bcc or β phase, space group Im-3m) at temperature above 1155 K [5] under ambient pressure. With increasing pressure at room temperature, the α phase transforms into hexagonal AlB_2 type structure called ω phase (space group P6/mmm). The α-ω transition, which is driven by the electron transfer from s to d band, is a representative example of martensitic transformations and has been observed to occur between 2 and 15 GPa at room temperature [6], depending on the experimental technique, the pressure environment, and the sample purity. The phase diagram of Ti was well investigated by Zhang *et al.* experimentally [7, 8]. By conducting synchrotron X-ray diffraction experiments, they derived thermal phase transformation and thermal equations of state of Ti under high temperature and high pressure. But the phase diagram of Ti has not been well studied theoretically due to the well-known soften phonon modes of the β-Ti. The phonon spectra reveal imaginary phonon frequencies of the soft modes in traditional QHA, indicating the dynamical instability. But the measured frequen-

*Author to whom correspondence should be addressed. E-mail: zhaoyizeng@126.com

cies of β-Ti are positive in experiments [9], because the anharmonic effects are neglected in QHA. Therefore the information on the temperature dependence of the vibrational modes and the phonon-phonon interactions that are responsible for the high temperature phase stability is lost. If we consider the phonon-phonon interactions, we can obtain the phonon dispersions at different temperatures and more accurate thermodynamic properties.

In this work, we extrapolated SCAILD method to high pressure and predicted the phase diagram of Ti under high temperature and high pressure. As the method contains the interaction between phonons, it can properly describe the dynamical stability and phase transition of Ti exactly.

II. COMPUTATIONAL METHOD

The calculations were performed using DFT and implemented through the Vienna *ab initio* simulation package. In the calculation, we used the highly accurate frozen core all-electron projector augmented wave (PAW) method [10]. The exchange and correlation potentials were treated within Perdew, Burke, and Ernzerhof [11]. Our calculations were performed with a cutoff energy of 500 eV, treating 3p, 3d, and 4s orbitals as valence states. For the static structural calculations, the 17×17×11, 11×11×17, and 19×19×19 Γ-centered k meshs were used for α-, ω-, and β-Ti, respectively. All necessary convergence tests were performed and the self-consistence convergence of the energy was set to 10^{-6} eV/atom. High temperature phonon calculations were performed using SCAILD method. We calculated 54, 81, and 64 atoms for α-, ω-, and β-Ti with Monkhorst-Pack 5×5×5 k-point grid and Fermi smearing in the calculations. The self-consistence convergence of the energy was set to 0.1 meV/atom. To obtain the force constants for the phonon calculations, atomic displacements of 0.03 Å were employed. The Helmholtz free energy F can be accurately separated as

$$F(V,T) = U_0(V) + F_{\rm phon}(V,T) + F_{\rm elec}(V,T) \quad (1)$$

where $U_0(V)$ is the energy of a static lattice at zero temperature, $F_{\rm elec}(V,T)$ is the thermal free energy arising from electronic excitations, and $F_{\rm phon}(V,T)$ is the phonon contribution. The temperature dependent parts of the free energy can be found as

$$F_{\rm phon}(V,T) + F_{\rm elec}(V,T) = \Delta F(\{U_R\},V,T) + \frac{3}{2}k_{\rm B}T - TS_{\rm ph}(V,T) \quad (2)$$

where $k_{\rm B}$ is the Boltzmann constant, U_R is the atomic displacements generated throughout the SCAILD self-consistent run. Here ΔF is the change in free energy relative to the ground-state energy U_0, caused by the phonon-induced atomic displacements, and thermal excitations of the electronic states. ΔF can be obtained by calculating the total free energy of the corresponding atomic configuration, $\{U_R\}$, using a Fermi-Dirac temperature smearing. $3k_{\rm B}T/2$ is the classical phonon kinetic energy per atom. $TS_{\rm ph}$ is the contribution of vibrational entropy, which can be estimated from the self-consistent density of states of the phonons $g(\nu,V)$ as follows

$$TS_{\rm ph}(V,T) = \int_0^\infty {\rm d}\omega g(\nu,V,T)\hbar\nu\left\{n\left(\frac{\hbar\nu}{k_{\rm B}T}\right) - \frac{k_{\rm B}T}{\hbar\nu}\ln\left[1-\exp\left(-\frac{\hbar\nu}{k_{\rm B}T}\right)\right]\right\} \quad (3)$$

where ν is the phonon frequency. More details about theoretical background can be found in the SCAILD method [4].

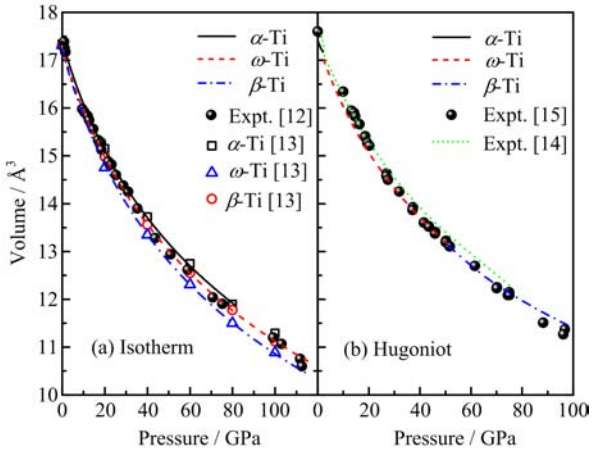

FIG. 1 EOS of Ti. (a) Isotherm at 0 K, together with experimental data [12] (solid spheres) and theoretical results [13] (open symbols). (b) Hugoniot of Ti, together with the experimental data [14, 15].

III. RESULTS AND DISCUSSION

The calculated static equilibrium volumes of α-, ω-, and β-Ti are 17.4, 17.1, and 17.2 Å^3, respectively. For α- and ω-Ti, the axial c/a ratios are 1.58 and 0.62, respectively. The static equation of state (EOS) of α-, ω- and β-Ti can be obtained from the static energy-volume (E-V) data. The calculated static isotherms of Ti are shown in Fig.1(a). Our results generally agree with the experimental data [12] and the theoretical results [13]. We also obtained the Hugoniot curve, which can reflect the response of material to both pressure and temperature. The $P_{\rm H}$-$V_{\rm H}$ (Fig.1(b)) at Hugoniot agrees well with the experiments [14, 15].

The finite temperature phonon dispersion curves of α-Ti along several high-symmetry directions are displayed in Fig.2 (a) and (b). At 0 GPa, the calculated 300 K phonon dispersions reproduce the overall trend of the inelastic-neutron-scattering measurement

DOI:10.1063/1674-0068/28/cjcp1411202

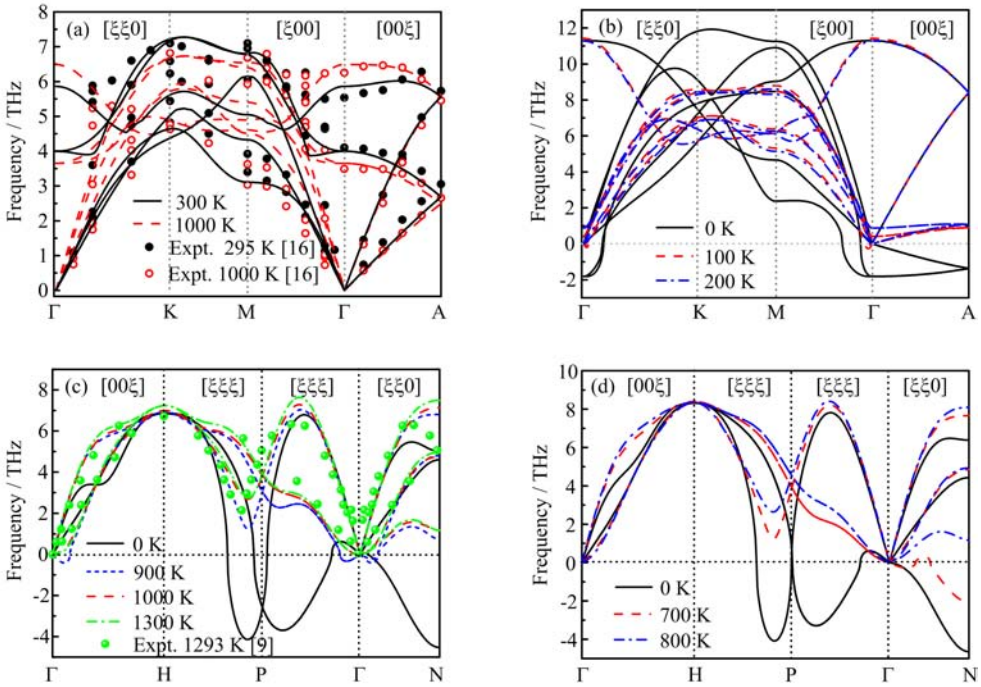

FIG. 2 Temperature phonon dispersion curves of Ti. (a) α-Ti at 0 GPa, (b) α-Ti at 53 GPa, (c) β-Ti at 0 GPa, and (d) β-Ti at 19 GPa.

by Stassis *et al.* [16]. As the temperature increases, the striking temperature effects can be seen by studying the low- and high-temperature phonon dispersions. The increased splitting between the longitudinal and transverse optic modes is captured. For the 1000 K modes, there are a little difference between the present phonon spectra and experimental data, *i.e.* along Γ-M-K-Γ, we overestimate the frequencies in acoustic branches. However, the agreements of the high-energy optical frequencies are quite good. We repeat the phonon calculations under different pressures and temperatures. At 0 K, all the optical frequencies increase with increasing pressure, except the acoustic frequencies. As pressure increases, the softening becomes more and more obvious. Under compression (above 36 GPa), the frequencies around the Γ point and along Γ-A in the transverse acoustical (TA) branches soften to imaginary frequencies, indicating the structural instability. When the temperature increases up to a critical temperature T_c, the imaginary frequencies are promoted to real under high pressure. Figure 2(b) shows the calculated phonons at 0, 100, and 200 K at 53 GPa. It is obvious that the SCAILD calculations predict the stability of α-Ti by promoting the frequencies from imaginary to real at temperatures 150±50 K. The phonon dispersios of ω-Ti at different temperatures and pressures are also obtained in present work. As all the phonon frequencies are positive in the calculated pressure and temperature range (0−100 GPa and 0−1500 K), and increase with the increasing pressure, which indicates the dynamical stability of ω-Ti, we do not show the calculated dispersions here.

For β-Ti, as a high temperature phase, its 0 K phonon dispersions should be unstable, just as is shown in Fig.2 (c) and (d). The soft mode around P point is responsible for the β to ω transformation, while the unstable phonon branch in the T-[110] direction corresponds to the β to α transformation [9]. By comparing the high temperature data with the 0 K data, it is obvious that each phonon frequency at high temperature suffers a shift due to the effects of anharmonicity. At 0 GPa, above 1000 K, the imaginary modes in the phonon dispersions are completly absent. The predicted 1300 K phonon dispersion of β-Ti agrees well with the experimental data measured at 1293 K [9]. Under 0 and 19 GPa, the predicted stability of β-Ti by promoting the frequencies of the phonons along the Γ-P-H and Γ-N symmetry line from imaginary to real for temperatures 950±50 and 750±50 K, respectively.

From the phonon dispersions, we can obtain some other information, such as the acoustic sound velocities, which can be obtained from the low spectra. In a cubic crystal, the acoustic velocities can be calculated for the longitudinal and transverse waves in the ⟨100⟩, ⟨111⟩, and ⟨110⟩ directions, using the following equation:

$$V = \frac{\mathrm{d}\nu}{\mathrm{d}\,|\mathbf{q}|} \tag{4}$$

where $\mathbf{q}$ is the wave vector. The harmonic elastic constant C_{ij} can be obtained by solving the following:

$$C_{11} = \rho V_{\mathrm{L}}^2 \tag{5}$$

DOI:10.1063/1674-0068/28/cjcp1411202

TABLE I The acoustic velocities and harmonic elastic constant for β-Ti under HPHT.

P/GPa	T/K	$V_{\rm L}$/(km/s)	$V_{\rm T1}$/(km/s)	$V_{\rm T2}$/(km/s)	C_{11}/GPa	C_{12}/GPa	C_{44}/GPa
0	1300	4.52	2.86	1.32	99.6	82.6	39.8
0 [9]	1273				97.7	82.7	37.5
19	800	5.87	2.83	1.53	184.7	140.8	42.8
	1000	5.84	2.80	1.59	182.8	136.6	41.7
	1200	5.81	2.76	1.85	180.8	128.6	40.9
43	600	7.01	2.85	1.47	290.2	219.9	48.0
	800	7.00	2.84	1.61	289.9	216.4	47.6
	1000	7.01	2.82	1.64	287.5	212.9	47.0
	1200	6.97	2.80	1.68	287.3	210.8	46.3
73	300	7.47	2.87	1.68	363.4	253.3	53.6
	600	7.46	2.86	1.73	363.1	251.1	53.3
	800	7.45	2.85	1.78	362.5	248.2	53.0
	1000	7.44	2.84	1.80	361.8	246.4	52.8
	1200	7.43	2.84	7.84	361.2	243.8	52.8

$$C_{44} = \rho V_{\rm T1}^2 \tag{6}$$

$$\frac{1}{2}(C_{11} - C_{12}) = \rho V_{\rm T2}^2 \tag{7}$$

where the wave velocities $V_{\rm L}$, $V_{\rm T1}$, $V_{\rm T2}$ correspond to longitudinal $\langle 100 \rangle$, transverse $\langle 100 \rangle$, and slow transverse $\langle 110 \rangle$ waves, respectively. For β-Ti, the calculated velocities $V_{\rm L}$, $V_{\rm T1}$, and $V_{\rm T2}$ at 1300 K are 4.52, 2.86, and 1.32 km/s, respectively. The extrapolated harmonic elastic constants for C_{11}, C_{12}, and C_{44} are 99.6, 82.6, and 39.8 GPa, which agree with the experimental data 97.7, 82.7, and 37.5 GPa at 1273 K. The more acoustic velocities and elastic constants are shown in Table I. The acoustic velocities increase with the increasing pressure and decrease with the increasing temperature, especially for $V_{\rm T2}$. It is noted that the variation of $V_{\rm T2}$ is a direct response of the phonon branch in the T-[110] direction, and it can reflect the stability of β phase. On the other hand, the predicted elastic constant C_{11} is larger than C_{12} at the given pressure and temperature state, which indicates β-Ti is mechanical stable.

Considering the dynamical stabilities of α-, ω-, and β-Ti, we can obtain the dynamical stable regions of α-, ω-, and β-Ti in the P-T phase diagram. As is shown in Fig.3, below 36 GPa, α-Ti is a dynamical stable phase. As pressure increases, $T_{\rm c}$ in which the unstable phase transforms to stable phase increases rapidly. The transition temperatures as functions of pressure can be described as a second polynomial:

$$T_{\rm c} = 1250 - 63.18P + 0.79P^2 \tag{8}$$

For ω-Ti, it is a dynamical stable phase in the entire calculated P-T region. For β-Ti, $T_{\rm c}$ decreases with the increasing pressure. A second polynomial can describe $T_{\rm c}$ as functions of pressure:

$$T_{\rm c} = 950 - 8.60P - 0.01P^2 \tag{9}$$

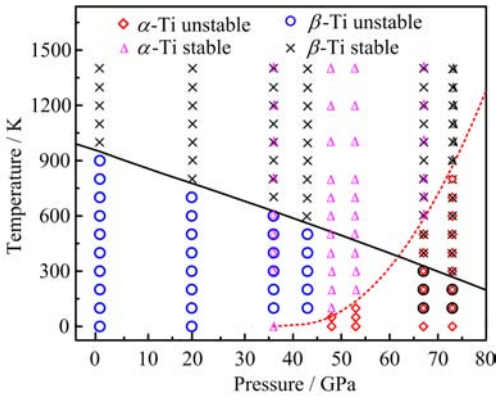

FIG. 3 Dynamic stability of Ti. Solid line and dashed line are fitted stable and unstable boundaries, respectively.

The phonon dispersion relations, while interesting, are not the main goal of this work. We want a solid method to deal with lattice dynamics for strongly anharmonic dynamically unstable systems. To test this, we calculated the Gibbs free energies of Ti. In Fig.4 we present the calculated phase diagram of Ti, together with other theoretic results [17, 18] and experimental data [8]. The transition temperatures of ω-α and α-β locate at 150±50 and 1150±50 K at zero pressure, which are a little larger than previous QHA data of 146 and 1143 K [19]. The predicted triple point locates at 8.8 GPa, 975 K, which is close to the experimental data of 9 GPa, 940 K [5]. The present results generally accord with previous QHA data [19]. The main difference is the slope ($\mathrm{d}T/\mathrm{d}P$) of the ω-β boundary. Considering the phonon-phonon interactions, the present slope is much larger than the results in QHA. The present slope of α-ω, α-β, and ω-β boundary are 94, −17, and 6 K/GPa, respectively. The Hugoniot $P_{\rm H}$-$T_{\rm H}$ curve is also shown in Fig.4. It can be seen that the shock

DOI:10.1063/1674-0068/28/cjcp1411202

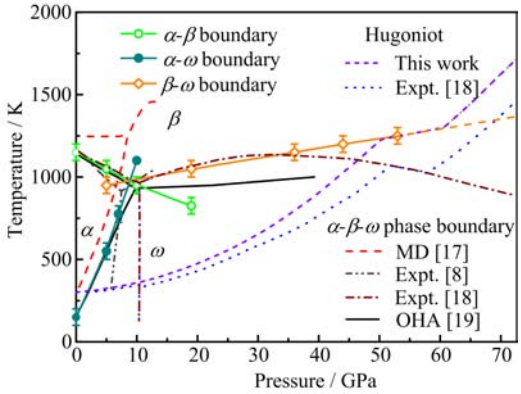

FIG. 4 Phase diagram of Ti under high-pressure and high-temperature.

induced α-ω transition locates at ∼2.2 GPa, which is smaller than the shock transition pressure ∼12 GPa [14]. The reason is that the hysteresis of the α-ω transformation is so great that the high pressure phase is retained after removal of the load. Application of shear stress is found to reduce the hysteresis of the transformation, allowing the equilibrium transition pressure at room temperature to be estimated at 2.0±0.3 GPa [20]. In α-ω transition, our results reveal a 0.9% volume reduction (shown in Fig.1(b)), which is a little smaller than the experimental data 1.2%. The small volume change in this transition is not surprised because both phases possess a hexagonal symmetry and similar atomic packing. As is shown in Fig.4, the Hugoniot traverses the β phase before crossing the melting curve and indicates the shock induced ω-β transition around 50−60 GPa and 1200−1300 K, which agree with the results of Kerley [18]. In the present work, there are no volume break can be observed in ω-β transition.

IV. CONCLUSION

We employ SCAILD methods to investigate the temperature dependent phonon spectra of Ti. In the calculations, the phonon-phonon interactions were considered. By reproducing the observed high temperature phonon frequencies at zero pressure with good accuracy, we predicted the high temperature phonons under high pressure, and obtained the critical temperature, in which the frequencies were promoted from imaginary to real. And then the stable regions of α-, ω-, and β-Ti were predicted successfully. From the phonon dispersions, we also extrapolated the acoustic velocities and harmonic elastic constants. By comparing the free energies, we obtained the Hugoniot and the phase diagram of Ti. Excellent agreement with experimental results in present simulations indicates the usefulness of the SCAILD method and it can be designed to work for much more strongly anharmonic systems where the traditional QHA fails.

V. ACKNOWLEDGMENTS

This work was supported by the National Natural Science Foundation of China (No.11304408 and No.1347019), the NSAF (No.U1230201), the Natural Science Foundation of Chongqing City (No.cstc2012jjA50019 and No.cstc2013jcyjA0733), the China Postdoctoral Science Foundation (No.2014M552380 and No.2014M552541XB).

[1] P. Souvatzis, D. Legut, O. Eriksson, and M. I. Katsnelson, Phys. Rev. B **81**, 092201 (2010).
[2] P. Souvatzis, O. Eriksson, M. I. Katsnelson, and S. P. Rudin, Phys. Rev. Lett. **100**, 095901 (2008).
[3] E. S. Božin, C. D. Malliakas, P. Souvatzis, T. Proffen, N. A. Spaldin, M. G. Kanatzidis, and S. J. L. Billinge, Science **330**, 1660 (2010).
[4] P. Souvatzis, S. Arapan, O. Eriksson, and M. I. Katsnelson, Eur. Phys. Lett. **96**, 66006 (2011).
[5] D. A. Young, *Phase Diagrams of the Elements*, Berkeley: University of California Press, (1991).
[6] D. Errandonea, Y. Meng, M. Somayazulu, and D. Hausermann, Physica B **355**, 116 (2005).
[7] J. Zhang, Y. Zhao, R. S. Hixson, G. T. Gray, L. P. Wang, W. Utsumi, S. Hiroyuki, and H. Takanori, Phys. Rev. B **78**, 054119 (2008).
[8] J. Zhang, Y. Zhao, R. S. Hixson, G. T. Gray, L. Wang, W. Utsumi, S. Hiroyuki, and H. Takanori, J. Phys. Chem. Solids **69**, 2559 (2008).
[9] W. Petry, A. Heiming, J. Trampenau, M. Alba, C. Herzig, H. R. Schober, and G. Vogl, Phys. Rev. B **43**, 10933 (1991).
[10] P. E. Blöchl, O. Jepsen, and O. K. Andersen, Phys. Rev. B **49**, 16223 (1994).
[11] J. P. Perdew, K. Burke, and M. Ernzerhof, Phys. Rev. Lett. **77**, 3865 (1996).
[12] Y. K. Vohra and P. T. Spencer, Phys. Rev. Lett. **86**, 3068 (2001).
[13] S. A. Ostanin and V. Y. Trubitsin, J. Phys.: Condens. Matter **9**, L491 (1997).
[14] C. W. Greeff, D. R. Trinkle, and R. C. Albers, J. Appl. Phys. **90**, 2221 (2001).
[15] S. P. Marsh, *Los Alamos Shock Hugoniot Data*, Berkeley: University of California Press, (1980).
[16] C. Stassis, D. Arch, and B. N. Harmon, Phys. Rev. B **19**, 181 (1979).
[17] R. G. Hennig, T. J. Lenosky, D. R. Trinkle, S. P. Rudin, and J. W. Wilkins, Phys. Rev. B **78**, 054121 (2008).
[18] G. I. Kerley, *Equations of State for Titanium and $Ti_6A_{14}V$ Alloy*, Sandia National Laboratories Report, No.SAND2003-3785, (2003).
[19] C. E. Hu, Z. Y. Zeng, L. Zhang, X. R. Chen, L. C. Cai, and D. Alfè, J. Appl. Phys. **107**, 093509 (2010).
[20] V. A. Zilbershtein, G. I. Nosova, and E. I. Estrin, Fiz. Met. Metalloved **35**, 584 (1973).

DOI:10.1063/1674-0068/28/cjcp1411202